Electronic Supplementary Material (ESI) for New Journal of Chemistry.

Post-synthetic modification of UiO-66-OH toward porous liquids for CO_2 capture

Yangyang Xin,†[a] Dechao Wang,†[a] Dongdong Yao, [a] Hailong Ning, [b] Xiaoqian Li, [a] Xiaoqian Ju, [b] Yichi Zhang, [a] Zhiyuan Yang, [b] Yahong Xu*[c] and Yaping Zheng*[a]

[a] School of Chemistry and Chemical Engineering, Northwestern Polytechnical University, Xi'an 710129, P. R. China.

[b] College of Chemistry and Chemical Engineering, Xi'an University of Science and Technology, Xi'an 710021, P. R. China.

[c]Key Laboratory for Light-weight Materials, Nanjing Tech University, Nanjing 210009, P. R. China.

* Corresponding authors. E-mail: 13701360679@163.com(Yahong Xu), zhengyp@nwpu.edu.cn (Yaping Zheng).

† They are co-first authors with the same contribution to the paper.

Table of Contents

1. Reaction between UiO-66-OH with KH550 and SID.

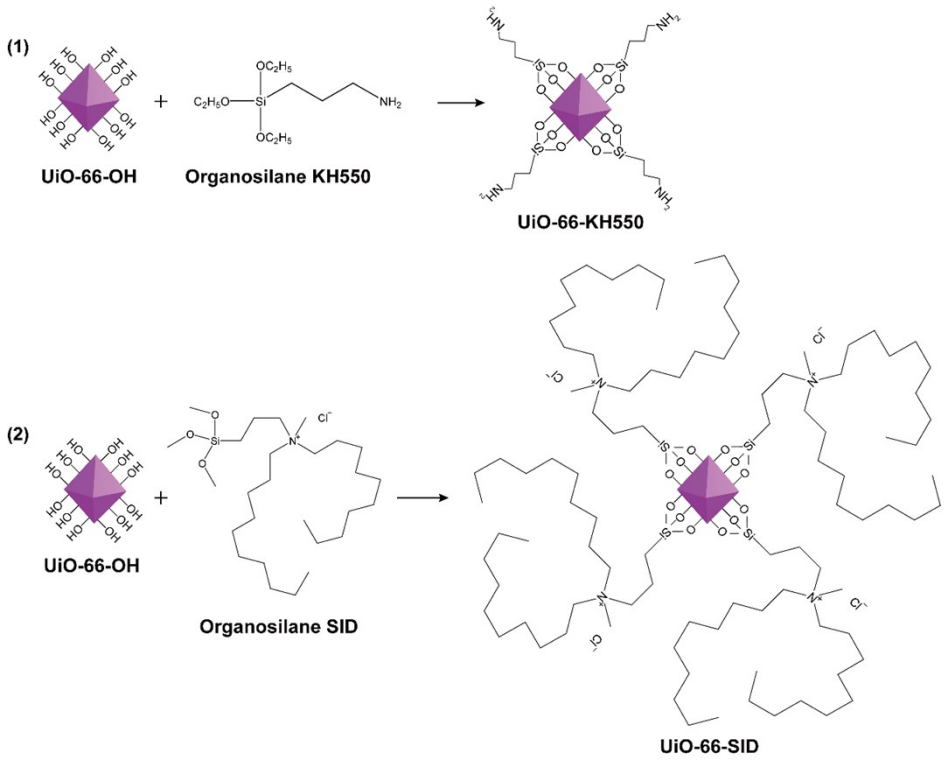

Figure S1. The reaction between UiO-66-OH with KH550 and SID.

2. Molecular Simulation

2.1 Molecular Structures Construction

The molecular structures of UiO-66 and PDMS were first established, and then the above structures were subjected to a geometric optimization process, followed by structural relaxation through a simulated annealing process. Then, the obtained low-energy conformations were further optimized by NVT molecular dynamics (MD) at 500-*ps* and NPT MD at 200-*ps*. The best structures obtained were used for the construction of porous liquid models in the following steps, and the model of UiO-66 is shown in **Figures S2a**.

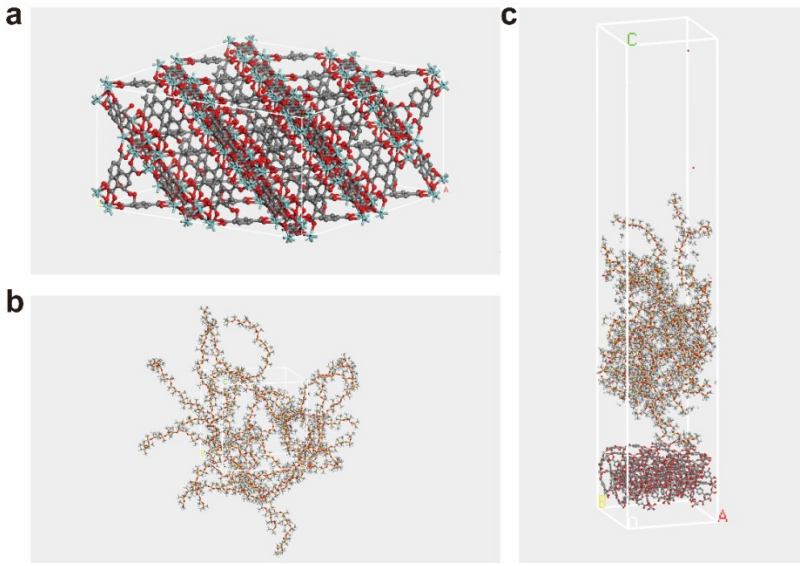

Figure S2. The molecular models of (a) UiO-66, (b) PDMS and (c) PL (for brevity, the H atom is deleted).

The molecular modeling of PDMS was performed using the *Amorphous Cell* (AC) module, and then the model went through geometry optimization, simulated annealing, and NVT kinetic processes for structural relaxation and relaxation in turn to obtain the low-energy conformation AC model of PDMS, and the constructed model is shown in **Figure S2b**. The initial density was set to 0.2 g/cm^3 at 25 °C [1]. Then, the optimization was carried out by geometric optimization pairs, and the local energy was minimized by the method of the *Smart* method, and the convergence accuracy was set to 0.00001 kcal/mol/Å. Subsequently, the obtained low-energy conformation was subjected to simulated annealing, and the temperature was increased from 25 °C to 327 °C. Then, it was cooled at an interval of 5 °C. Then a 500-*ps* relaxation of the NVT kinetic structure was performed, where the time step was 1 fs, and a Nose thermostat was used to control the temperature [2]. The equations of motion were integrated by the velocity Verlet algorithm with time steps of 1 fs for all simulation

runs. 0.001 kcal/mol was used as the convergence criterion by the atom-based method.

Finally, the porous liquid model was constructed using PDMS as sterically hindered solvents and UiO-66 as the pore generator.by Build Layers tool (**Figure S2c**). Then the lower bottom surface of UiO-66 was cut and a certain vacuum layer was set in the upper plane of PDMS to create an independent porous liquid system, and then the model was subjected to NVT dynamics of 500-*ps* to obtain the trajectory file to analyze the mutual interaction of PDMS sterically hindered solvent and UiO-66 in the porous liquid.

2.2 Force Fields

PDMS6000 was modeled and analyzed using COMPASS II force field (condensed phase optimized molecular potential for atomic simulation studies) with the following parameter settings (Equation S1) and validated using condensed phase properties, widely used for polymer, organic and inorganic material simulations.

$$\mathrm{E}=\sum_{b}\left[K_2\left(b-b_0\right)^2+K_3\left(b-b_0\right)^3+K_4\left(b-b_0\right)^4\right]+\sum_{\theta}\left[H_2\left(\theta-\theta_0\right)^2+H_3\left(\theta-\theta_0\right)^3+H_4\left(\theta-\theta_0\right)^4\right]$$

(a) (b)

$$+\sum_{\phi}\left\{V_1\left[1-\cos\left(\phi-\phi_1^0\right)\right]+V_2\left[1-\cos\left(2\phi-\phi_2^0\right)\right]+V_3\left[1-\cos\left(2\phi-\phi_3^0\right)\right]\right\}$$

(c)

$$+\sum_{\chi}K_{\chi}\chi^2+\sum_{b}\sum_{b'}F_{bb'}\left(b-b_0\right)\left(b'-b_0'\right)+\sum_{\theta}\sum_{\theta'}F_{\theta\theta'}\left(\theta-\theta_0\right)\left(\theta'-\theta_0'\right)$$

(d) (e)

$$+\sum_{b}\sum_{\theta'}F_{b\theta}\left(b-b_0\right)\left(\theta-\theta_0\right)+\sum_{b}\sum_{\phi}\left(b-b_0\right)\left[V_1\cos\phi+V_2\cos 2\phi+V_3\cos 3\phi\right]$$

(f) (g)

$$+\sum_{b'}\sum_{\phi}\left(b'-b_0'\right)\left[V_1\cos\phi+V_2\cos 2\phi+V_3\cos 3\phi\right]$$

(h)

$$+\sum_{\phi}\sum_{\theta}\sum_{\theta'}K_{\phi\theta\theta'}\cos\phi\left(\theta-\theta_0\right)\left(\theta'-\theta_0'\right)+\sum_{i>j}\frac{q_iq_j}{\varepsilon r_{ij}}+\sum_{i>j}\left[2\left(\frac{A_{ij}}{r_{ij}^9}\right)-3\left(\frac{B_{ij}}{r_{ij}^6}\right)\right] \quad \text{(S1)}$$

(j) (k) (l)

Among them, the energy terms are divided into three categories: bonding energy terms, cross terms, and non-bonding energy terms, respectively. The bonding energy consists of three components: (a) the covalent bond stretching energy term, (b) the bonding angle bending energy term, and (c) the torsion angle rotation energy term of the polymer chain. The out-of-plane energy, or anomalous term (d), is described as a harmonic function. The cross-interaction terms include the dynamics of bond stretching, bending, and torsional angular rotation (e-j). The last two terms (k) and (l) represent the Coulomb electrostatic force and the van der Waals force, respectively.

The model construction and analysis of UiO-66 use the Universal force field, which is a universal force field that has been widely used in the modeling and analysis process of rigid materials with MOFs [3].

2.3 Fractional Accessible Volume (FAV) Analysis

The fractional accessible volume (FAV) is the locus of the probe center as the probe freely rolls over the framework [4]. A gas molecule probe is randomly inserted into the simulation box and the insertion is considered to be successful if the probe does not overlap with any polymer atom. In the calculation process, N_2 molecule was chosen as the molecule probe. The ratio of successful insertion to the total number of insertions gives FAV. Therefore, it is a reasonable method to determine the changes

of free accessible volume. In this study, FAV for constructed cells was obtained using the “Connolly surface” from the *Visualizer* module [5].

3. CO_2 sorption test device

First, complete the test parameter settings (test temperature and test pressure). Then, the exhaust valve is turned on through the automatic control system, and the target gas enters the reference cavity. When the pressure reaches the set value, record the pressure P1 of the reference chamber. Next, valve V1 is opened, and the target gas enters the sample cell and is adsorbed by the sample. When the adsorption equilibrium is reached, record the pressure P2 of the reference chamber. The automatic control and data recording system analyzes and records the equilibrium adsorption capacity according to the pressure change of the reference cavity.

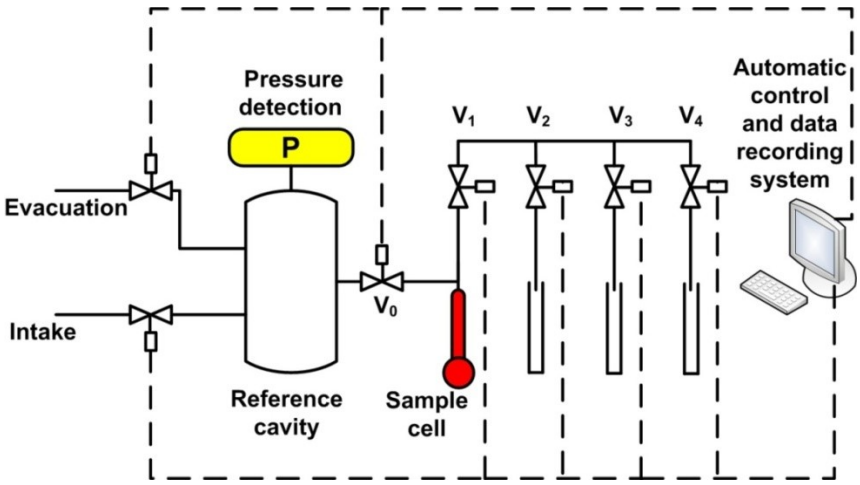

Figure S3. Schematic diagram of the high-temperature and high-pressure adsorption instrument analyzer: V0: pressure test valve; V1: desorption valve; V2: free valve; V3: desorption collection valve; V4: exhaust valve.

4. Data Analysis

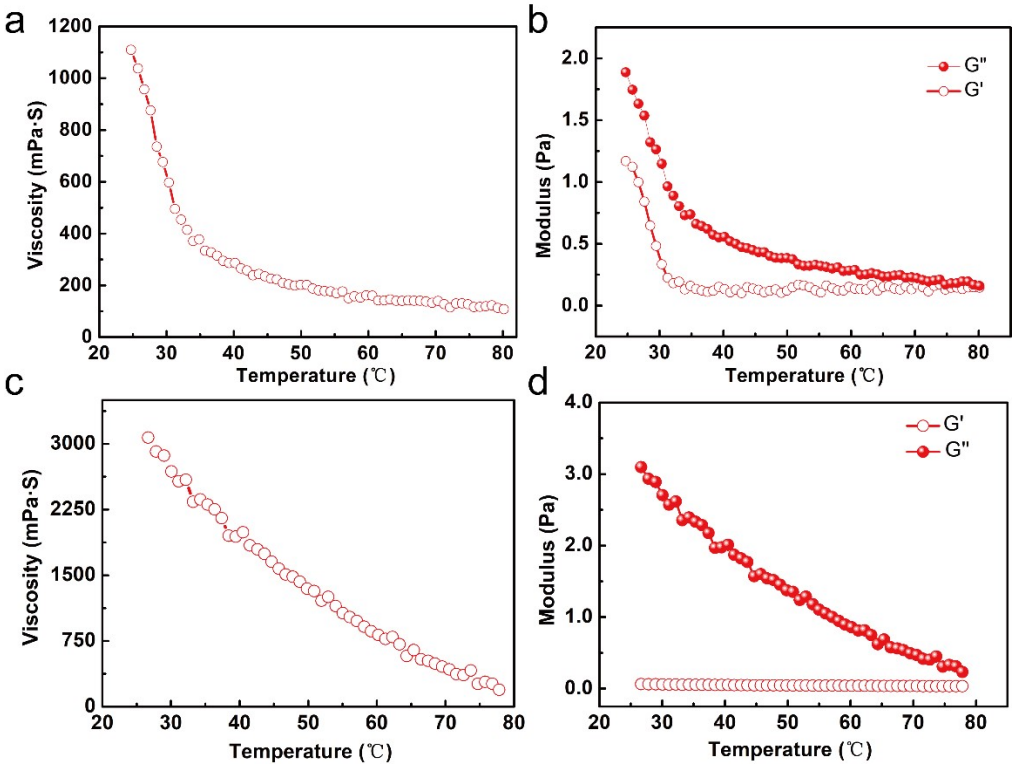

Figure S4. (a, c) Modulus-temperature curves of UiO-66-KH550-PDMS400 and UiO-66-KH550-PDMS6000. (d, f) Viscosity-temperature curves of UiO-66-KH550-PDMS400 and UiO-66-KH550-PDMS6000.

Table S1. The summary of reported PLs together with corresponding porous generators, sterically hindered solvents and their viscosities according to previous studies.

Common name	Porous generators	Hindered solvents	Type	Viscosities (Pa·S at 25 °C)	Ref.

HS PL	Hollow Silica	PEGS	I	6.8 (40 °C)	[6]
HS PL	HS	Organosilane and oligomer	I	0.66	[7]
UiO-66-OH PLs	UiO-66-OH	Polyether amine	I	14.0	[8]
MOF liquids	ZIF-4	NA	I	8.0 (567 °C)	[9]
POC PLs	CC15-R	Hexachloropropene	III	4.18	[10]
UiO-66 PL	D2000@UiO-66	[M2070][IPA]	III	4.0	[11]
ZIF-based PL	ZIF-67	$[C_6BIm_2][NTf_2]$	III	0.54	[12]
UiO-66-liquid-M2070 PL	UiO-66	Organosilane and oligomer	III	4.5	[13]
MOF PL	UiO-66@PDMS	PDMS	III	6.0	[14]
Zeolites PL	Zeolites	$[P_{6,6,6,14}][Br]$	III	9.55	[15]
MOF PL	ZIF-67	N-heterocyclic carbene ligands	III	0.16	[16]
POC PL	Crown-ether cage	CH_3Cl PCP	III	0.02	[17]
ZIF-8/Water PL	ZIF-8	Water	III	0.013	[18]

NA= not available

Table S2. Comparison of CO_2 uptake performance of reported PLs in previous studies.

Sample names	CO_2 uptake (mmol/g)	Testing conditions	Ref.
ZIF-8 PLs	1.60	298 K, 10 bar	[19]
Hollow silica PLs	0.9	298 K, 10 bar	[7]
15-C-5 PL	0.38	298 K, 10 bar	[20]
18-C-6-PL	0.43	298 K, 5 bar	[20]
PAF-1/Genosorb PLs	0.72	298 K, 5 bar	[21]
Al(fum) (OH)/PDMS PLs	0.95	298 K, 5 bar	[21]

Scrambled cage CC3-R/(HCP)	0.055	298 K, 10 bar	[22]
UiO-66 PLs	1.66	298 K, 10 bar	[11]
H-ZSM-5 PLs	0.46	298 K, 10 bar	[23]
Porous carbons liquids	0.56	298 K, 10 bar	[15]
UiO-66-liquid	0.86	298 K, 30 bar	[8]

Refenences

[1] K. Golzar, S. Amjad-Iranagh, M. Amani, H. Modarress, Molecular Simulation Study of Penetrant Gas Transport Properties into the Pure and Nanosized Silica Particles Filled Polysulfone Membranes, J Membrane Sci, 451 (2014) 117-134.

[2] M. Pazirofteh, M. Dehghani, S. Niazi, A.H. Mohammadi, M. Asghari, Molecular Dynamics Simulation and Monte Carlo Study of Transport and Structural Properties of Peba 1657 and 2533 Membranes Modified by Functionalized Poss-Peg Material, Journal of Molecular Liquids, 241 (2017) 646-653.

[3] A.K. Rappe, C.J. Casewit, K.S. Colwell, W.A. Goddard, W.M. Skiff, Uff, a Full Periodic Table Force Field for Molecular Mechanics and Molecular Dynamics Simulations, Journal of the American Chemical Society, 114 (1992) 10024-10035.

[4] R.L.C. Akkermans, N.A. Spenley, S.H. Robertson, Monte Carlo Methods in Materials Studio, Molecular Simulation, 39 (2013) 1153-1164.

[5] M.L. Connolly, Computation of Molecular Volume, Journal of the American Chemical Society, 107 (1985) 1118-1124.

[6] J. Zhang, S.H. Chai, Z.A. Qiao, S.M. Mahurin, J. Chen, Y. Fang, S. Wan, K. Nelson, P. Zhang, S. Dai, Porous Liquids: A Promising Class of Media for Gas Separation, Angew Chem Int Ed Engl, 54 (2015) 932-

936.

[7] T. Shi, Y. Zheng, T. Wang, P. Li, Y. Wang, D. Yao, Effect of Pore Size on the Carbon Dioxide Adsorption Behavior of Porous Liquids Based on Hollow Silica, Chemphyschem, 19 (2018) 130-137.

[8] D. Wang, Y. Xin, X. Li, H. Ning, Y. Wang, D. Yao, Y. Zheng, Z. Meng, Z. Yang, Y. Pan, P. Li, H. Wang, Z. He, W. Fan, Transforming Metal-Organic Frameworks into Porous Liquids via a Covalent Linkage Strategy for CO_2 Capture, ACS Appl Mater Interfaces, 13 (2021) 2600-2609.

[9] R. Gaillac, P. Pullumbi, K.A. Beyer, K.W. Chapman, D.A. Keen, T.D. Bennett, F.-X. Coudert, Liquid Metal–Organic Frameworks, Nature Materials, 16 (2017) 1149-1154.

[10] B.D. Egleston, K.V. Luzyanin, M.C. Brand, R. Clowes, M.E. Briggs, R.L. Greenaway, A.I. Cooper, Controlling Gas Selectivity in Molecular Porous Liquids by Tuning the Cage Window Size, Angew Chem Int Ed Engl, 59 (2020) 7362-7366.

[11] X. Zhao, Y. Yuan, P. Li, Z. Song, C. Ma, D. Pan, S. Wu, T. Ding, Z. Guo, N. Wang, A Polyether Amine Modified Metal Organic Framework Enhanced the CO_2 Adsorption Capacity of Room Temperature Porous Liquids, Chem Commun (Camb), 55 (2019) 13179-13182.

[12] X. Li, D. Wang, Z. He, F. Su, N. Zhang, Y. Xin, H. Wang, X. Tian, Y. Zheng, D. Yao, M. Li, Zeolitic Imidazolate Frameworks-Based Porous Liquids with Low Viscosity for CO_2 and Toluene Uptakes, Chemical Engineering Journal, 417 (2021) 129239.

[13] D. Wang, Y. Xin, X. Li, F. Wang, Y. Wang, W. Zhang, Y. Zheng, D. Yao, Z. Yang, X. Lei, A Universal Approach to Turn UiO-66 into Type 1 Porous Liquids via Post-Synthetic Modification with Corona-Canopy Species for CO_2 Capture, Chemical Engineering Journal, 416 (2021) 127625.

[14] S. He, L. Chen, J. Cui, B. Yuan, H. Wang, F. Wang, Y. Yu, Y. Lee, T. Li, General Way to Construct Micro- and Mesoporous Metal-Organic Framework-Based Porous Liquids, J Am Chem Soc, 141 (2019) 19708-

19714.

[15] P. Li, H. Chen, J.A. Schott, B. Li, Y. Zheng, S.M. Mahurin, D. Jiang, G. Cui, X. Hu, Y. Wang, L. Li, S. Dai, Porous Liquid Zeolites: Hydrogen Bonding-Stabilized H-ZSM-5 in Branched Ionic Liquids, Nanoscale, 11 (2019) 1515-1519.

[16] A. Knebel, A. Bavykina, S.J. Datta, L. Sundermann, L. Garzon-Tovar, Y. Lebedev, S. Durini, R. Ahmad, S.M. Kozlov, G. Shterk, M. Karunakaran, I.D. Carja, D. Simic, I. Weilert, M. Klüppel, U. Giese, L. Cavallo, M. Rueping, M. Eddaoudi, J. Caro, J. Gascon, Solution Processable Metal–Organic Frameworks for Mixed Matrix Membranes Using Porous Liquids, Nature Materials, 19 (2020) 1346-1353.

[17] N. Giri, M.G. Del Pópolo, G. Melaugh, R.L. Greenaway, K. Rätzke, T. Koschine, L. Pison, M.F.C. Gomes, A.I. Cooper, S.L. James, Liquids with Permanent Porosity, Nature, 527 (2015) 216-220.

[18] W. Chen, E. Zou, J.Y. Zuo, M. Chen, M. Yang, H. Li, C. Jia, B. Liu, C. Sun, C. Deng, Q. Ma, L. Yang, G. Chen, Separation of Ethane from Natural Gas Using Porous ZIF-8/Water-Glycol Slurry, Industrial & Engineering Chemistry Research, 58 (2019) 9997-10006.

[19] W. Shan, P.F. Fulvio, L. Kong, J.A. Schott, C.-L. Do-Thanh, T. Tian, X. Hu, S.M. Mahurin, H. Xing, S. Dai, New Class of Type Iii Porous Liquids: A Promising Platform for Rational Adjustment of Gas Sorption Behavior, ACS Applied Materials & Interfaces, 10 (2018) 32-36.

[20] N. Giri, C.E. Davidson, G. Melaugh, M.G. Del Pópolo, J.T.A. Jones, T. Hasell, A.I. Cooper, P.N. Horton, M.B. Hursthouse, S.L. James, Alkylated Organic Cages: From Porous Crystals to Neat Liquids, Chemical Science, 3 (2012) 2153-2157.

[21] J. Cahir, M.Y. Tsang, B. Lai, D. Hughes, M.A. Alam, J. Jacquemin, D. Rooney, S.L. James, Type 3 Porous Liquids Based on Non-Ionic Liquid Phases – a Broad and Tailorable Platform of Selective, Fluid Gas Sorbents, Chemical Science, 11 (2020) 2077-2084.

[22] D. Umeyama, S. Horike, M. Inukai, T. Itakura, S. Kitagawa, Reversible Solid-to-Liquid Phase Transition of Coordination Polymer Crystals, Journal of the American Chemical Society, 137 (2015) 864-870.

[23] P. Li, J.A. Schott, J. Zhang, S.M. Mahurin, Y. Sheng, Z.-A. Qiao, X. Hu, G. Cui, D. Yao, S. Brown, Y. Zheng, S. Dai, Electrostatic-Assisted Liquefaction of Porous Carbons, 56 (2017) 14958-14962.